

What does the instantaneous normal mode spectrum tell us about dynamical heterogeneity in glass-forming fluids?

Cite as: J. Chem. Phys. **151**, 184904 (2019); <https://doi.org/10.1063/1.5127821>

Submitted: 13 September 2019 . Accepted: 23 October 2019 . Published Online: 14 November 2019

Wengang Zhang , Jack F. Douglas , and Francis W. Starr 

COLLECTIONS

 This paper was selected as an Editor's Pick



View Online



Export Citation



CrossMark

Lock-in Amplifiers
... and more, from DC to 600 MHz



What does the instantaneous normal mode spectrum tell us about dynamical heterogeneity in glass-forming fluids?

Cite as: J. Chem. Phys. 151, 184904 (2019); doi: 10.1063/1.5127821

Submitted: 13 September 2019 • Accepted: 23 October 2019 •

Published Online: 14 November 2019



View Online



Export Citation



CrossMark

Wengang Zhang,^{1,2,a)}  Jack F. Douglas,^{1,b)}  and Francis W. Starr^{2,c)} 

AFFILIATIONS

¹Materials Science and Engineering Division, National Institute of Standards and Technology, Gaithersburg, Maryland 20899, USA

²Department of Physics, Wesleyan University, Middletown, Connecticut 06459, USA

^{a)}Electronic mail: wzhang01@wesleyan.edu

^{b)}Electronic mail: jack.douglas@nist.gov

^{c)}Electronic mail: fstarr@wesleyan.edu

ABSTRACT

We examine the instantaneous normal mode spectrum of model metallic and polymeric glass-forming liquids. We focus on the localized modes in the unstable part of the spectrum [unstable localized (UL) modes] and find that the particles making the dominant contribution to the participation ratio form clusters that grow upon cooling in a fashion similar to the dynamical heterogeneity in glass-forming fluids, i.e., highly mobile (or immobile) particles form clusters that grow upon cooling; however, a comparison of the UL mode clusters to the mobile and immobile particle clusters indicates that they are *distinct* entities. We also show that the cluster size provides an alternate method to distinguish localized and delocalized modes, offering a significant practical advantage over the finite-size scaling approach. We examine the trajectories of particles contributing most to the UL modes and find that they have a slightly enhanced mobility compared to the average, and we determine a characteristic time quantifying the persistence time of this excess mobility. This time scale is proportional to the structural relaxation time τ_α of the fluid, consistent with a prediction by Zwanzig [Phys. Rev. **156**, 190 (1967)] for the lifetime of collective excitations in cooled liquids. Evidently, these collective excitations serve to facilitate relaxation but do not actually participate in the motion associated with barrier crossing events governing activated transport. They also serve as a possible concrete realization of the “facilitation” clusters postulated in previous modeling of glass-forming liquids.

Published under license by AIP Publishing. <https://doi.org/10.1063/1.5127821>

I. INTRODUCTION

Because of the quasi-solid nature of glass-forming fluids, it has long been attractive to consider whether theoretical approaches used to describe the dynamics of crystalline solids could be adapted to understand the dynamics of glass-forming liquids. Formally, the normal modes of crystalline materials are quantified by the local curvature of the potential energy surface (PES) in the vicinity of the potential minimum, defining the crystalline solid state at zero temperature, where a harmonic approximation is commonly a good approximation. In contrast, liquids and crystals (at elevated temperatures approaching the melting temperature T_m) are able to explore

a much more complex PES. These systems can sample many minima and saddle points, connecting them so that extending the normal mode approach from ideal crystalline solids to real materials requires the incorporation of features of the local PES curvature from all regions explored by the material. Specifically, there are a significant number of directions in which the local curvature of the PES is negative in liquids and heated crystals, so many real materials exhibit a relatively “chaotic” dynamics not constrained to reside near the vicinity of potential energy minima. These local curvatures define the “instantaneous normal modes” (INMs) of the material,^{1–3} and below, we confine our attention to liquids in which the material system spends an appreciable time in the vicinity of both saddle

points and minima of the PES. There have been many attempts to develop a formal theory of liquid dynamics based on the INM approach, but quantitatively predictive results have generally been restricted to time scales on the order of local vibrational motions (i.e., picoseconds).^{4–8}

On the other hand, there has been progress in developing a formal theory for liquid diffusion based on a subset of the INM spectrum.^{9,10} The directions of negative curvature are commonly referred to as “unstable” modes, since they lead away from local minima, and correspondingly, these modes are naturally supposed to be related to diffusion in the liquid.¹¹ That said, the negative curvatures can also arise from anharmonicities of the PES, and so only a fraction of the unstable modes contributes significantly to diffusion and relaxation.^{2,12,13} Many early efforts attempted to “separate the wheat from the chaff” or, in other words, to identify those unstable modes that relate specifically to diffusion. In particular, there has been focus on the unstable modes that connect different local minima in configurational space (double-well modes).^{14–21} Alternatively, Bembenek and Laird^{2,13} proposed the method of filtering the unstable modes by examining the fraction of the system participating in the mode and argued that only those unstable modes that are delocalized (all particles participating) relate to diffusion, while localized modes (in which only a fraction participates significantly) are not relevant for diffusion. One significant challenge in pursuing this proposal has been the unambiguous separation of modes into localized and delocalized categories,^{2,13,22,23} a problem which was recently solved¹¹ by drawing upon ideas developed to quantify Andersen localization in classical dynamical systems based on random matrix theory.²⁴

The proposal that diffusion is controlled mainly by unstable delocalized (UD) modes does not address the fact that glass-forming liquids are “dynamically heterogeneous,”^{25–28} suggesting that *localized* unstable modes might play an important role in relaxation and diffusion, at least at low temperatures. In particular, simulations have indicated that molecules or segments of molecules within the fluid form long-lived clusters of relatively low or high mobility and mobile particle clusters can be further decomposed into string-like replacement motion, the size of which appears to govern relaxation processes in cooled liquids.^{29–32} Both high and low mobility clusters grow upon cooling toward the glass transition temperature T_g , where they appear to form interpenetrating networks of “fast” and “slow” particles.^{30,33–39} The rate of growth of these dynamical structures upon cooling clearly plays an important role in the glass transition, and this phenomenon is widely believed to be the origin of the decoupling between viscous and diffusive relation (i.e., the breakdown of the Stokes-Einstein relationship).⁴⁰ Given these observations, it is apparent that these heterogeneous motions do not correspond to modes that extend throughout the system, and thus, these motions might more naturally relate to those unstable modes arising from only a finite fraction of the fluid particles, i.e., localized modes.

The present work is an attempt to understand the nature of these unstable localized (UL) modes and to examine the degree to which these modes may relate to the dynamical heterogeneity mentioned above. In doing so, we are influenced by pioneering work by Zwanzig,⁴¹ indicating that collective transverse momentum excitations can be defined in liquids whose lifetime should scale in proportion to the fluid structural relaxation time (shear stress

relaxation time). We find that particles that contribute most to the UL modes form clusters, where the size of these clusters grows upon cooling, as found before for both mobile and immobile particle clusters characterizing dynamical heterogeneity in cooled liquids.³⁰ Moreover, the particles participating in the UL modes exhibit an enhanced mobility that persists on a time scale that scales in proportion to the structural relaxation time from the intermediate scattering function, in accord with Zwanzig’s theory, if these dynamical clusters are identified with fluid collective excitations. Perhaps surprisingly, the clusters of particles corresponding to the UL modes *do not* coincide with either the “mobile” or “immobile” clusters, identified previously in the study of mobility fluctuation in glass-forming liquids. Instead, these INM clusters seem to lie in the *boundary regions* between these extreme mobility clusters so that UL clusters are *facilitators* of the dynamics. We thus have another form of “dynamical heterogeneity” that is of interest for understanding the dynamics of glass-forming liquids from a fundamental perspective. Recent simulations have indicated a three-state structural heterogeneity in strongly interacting two-dimensional fluids that might be related to the three dynamical states observed in our simulations.⁴² A valuable side result is that we demonstrate that the cluster size can be used to discriminate between localized and delocalized modes, which is far less computationally intensive than the traditional finite-size scaling method to distinguish mode types.

We also mention that mobile facilitation clusters are a central feature of the model of glass-formation developed by Chandler and co-workers,⁴³ although it has not been clear how such clusters might be specified in structural glass-forming liquids. Kawasaki and Onuki^{44,45} have previously suggested kinds of facilitating particles that they term “bystander” particles that mediate the collective particle motion of the cooled liquid, and Zhang *et al.*⁴⁶ confirmed the indirect participation of relatively mobile particles in facilitating collective particle exchange motion. However, the significance of these “bystander” particles was not understood in these previous works.

The UL clusters offer a potential realization of such “facilitation” clusters. These findings are based on simulations of both a coarse-grained polymer model and the Kob-Andersen binary Lennard-Jones (BLJ) of Ni-P metallic glass⁴⁷ to demonstrate the robust nature of the results. It should be appreciated that the Kob-Andersen model is metastable with respect to the crystal,⁴⁷ so this is a model of a supercooled liquid at temperatures below the melting temperature of this system. Our polymer model apparently has not been observed to crystallize at low temperatures, enabling the study of the approach to glass-formation without the complication of incipient crystallization.

II. MODELING AND SIMULATION DETAILS

Our results are based on equilibrium molecular dynamics simulations of the bulk BLJ mixture⁴⁸ and bulk coarse-grained “spring-bead” polymer model.⁴⁹ Both polymer and BLJ simulations have been described in detail in earlier works.^{11,30}

The bulk BLJ contains 80% of type A particles and 20% of type B particles with the same mass. The interactions between these particles are the LJ potential,

$$V_{\alpha\beta}(r) = 4\epsilon_{\alpha\beta} \left[\left(\frac{\sigma_{\alpha\beta}}{r} \right)^{12} - \left(\frac{\sigma_{\alpha\beta}}{r} \right)^6 \right], \quad r < 2.5\sigma_{\alpha\beta}, \quad (1)$$

where $\alpha, \beta \in \{A, B\}$ with $\epsilon_{AA} = 1.0$, $\sigma_{AA} = 1.0$, $\epsilon_{AB} = 1.5$, $\sigma_{AB} = 0.8$, $\epsilon_{BB} = 0.5$, and $\sigma_{BB} = 0.88$. We employ periodic boundary conditions in all dimensions at a fixed density ($\rho = 1.204$) for all BLJ simulations. The temperature range we cover is $0.44 < T < 2.5$. This system and the thermodynamic path have been explored in countless previous publications, making it a natural first test case. We simulate BLJ with system sizes of 200, 400, 800, 1000, 1600, and 9000 particles; the system with 9000 particles is new to this work, while the smaller systems were simulated in Ref. 11.

The polymer melt consists of chains of 20 monomers linked by a finite extensible nonlinear elastic (FENE) spring potential. The FENE interaction parameters are $k = 30\epsilon$ and $R_0 = 1.5\sigma$. The interactions between all monomers are the forced-shifted Lennard-Jones (LJ) potential with $\sigma_{\text{poly}} = 1.0$ and $\epsilon_{\text{poly}} = 1.0$, truncated at $2.5\sigma_{\text{poly}}$. We consider systems containing either 100, 200, or 400 chains of polymer molecules. The temperature range we simulate for the bulk polymer is $0.30 < T < 2.5$. All polymer simulations are performed with periodic boundary conditions at constant density $\rho = 1.0$.

All quantities reported here are in reduced LJ units. The length is in terms of $\sigma \equiv \sigma_{AA} = 1.0$; energy is in terms of $\epsilon \equiv \epsilon_{\text{poly}} = 1.0$. Temperature is given in units of ϵ/k_B , where k_B is Boltzmann's constant. Time has the unit of $(m\sigma^2/\epsilon)^{1/2}$.

III. RESULTS AND DISCUSSION

A. INM and domains of vibrational spectrum

In order to examine the properties of the unstable localized modes, we need to first formally define the instantaneous normal modes. We start from the Hessian matrix that characterizes the curvatures of the local potential energy surface. The Hessian is a $3N \times 3N$ matrix, defined as

$$H_{i\alpha, j\beta} = \frac{\partial^2 V}{\partial r_{i\alpha} \partial r_{j\beta}}, \quad (2)$$

where i and j are particle indices and α and β are indices for the spatial direction. In the context of solids, the motion of the system can be viewed as quasiharmonic vibrations about the local potential energy minima. In this approximation, the eigenvalues λ_n of the Hessian matrix are obtained by solving the eigenvalue problem,

$$H\mathbf{e}_n = \lambda\mathbf{e}_n; \quad \lambda_n = m\omega_n^2, \quad (3)$$

where ω_n are the mode frequencies, m is the particle mass, and \mathbf{e}_n are the corresponding eigenvectors describing the mode motion. Since the liquid is not constrained to reside near a minimum of potential energy, the local curvature of the PES (and hence the force constant) can be negative. In the harmonic picture of motion, this corresponds to an imaginary mode frequency, corresponding to exponentially divergent motion. This is the reason why these imaginary modes are proposed to connect to molecular diffusion, as opposed to a simple restoring force. Following a standard practice, we represent imaginary frequencies $i\omega$ (associated with negative eigenvalues λ) as negative frequencies $-\omega$ to simplify the graphical presentation of the mode spectrum. We then evaluate the density of states (DOS) $\langle \rho(\omega) \rangle$ for both bulk BLJ and bulk polymer in Fig. 1, which is averaged over 100 independent configurations for each T . We exclude three zero frequency modes from the eigenfrequencies, since these modes correspond to a trivial translation of the system. Figure 1 shows that the fraction of the unstable modes decreases with decreasing temperature for both BLJ and polymer, indicated by the shrinking size of the negative lobe of DOS upon cooling. In contrast, compared to DOS of BLJ, we observe an additional feature in the high-frequency stable region of the spectrum in the bulk polymer [Fig. 1(b)], which is associated with the bonds that connect the nearest monomers within polymer chains.

To examine the spatial and temporal correlations of particles in different parts of the vibrational spectrum, we first need to unambiguously pinpoint the crossover point between the localized and delocalized modes in the vibrational spectrum. Clapa *et al.*¹¹ introduced a finite-size scaling approach to identify this crossover point. First, we replicate this method and then consider a new method focusing on the size of particle clusters that are

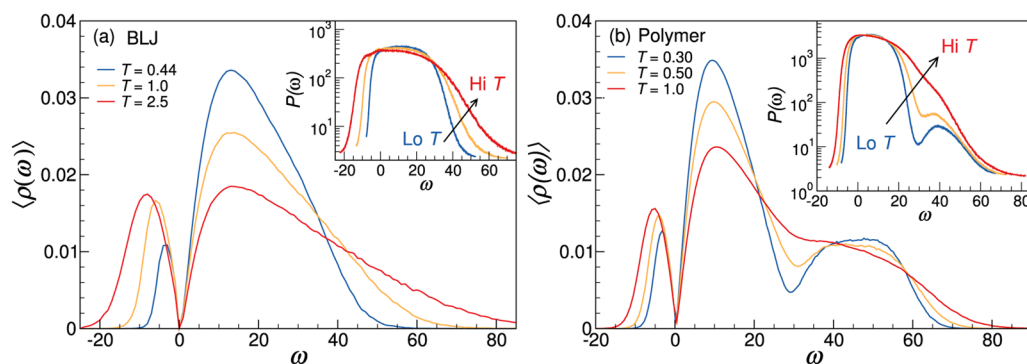


FIG. 1. The instantaneous normal mode density of states $\langle \rho(\omega) \rangle$ of (a) bulk binary Lennard-Jones mixture and (b) bulk polymer for some representative temperatures. The negative frequency ω represents the imaginary eigenfrequencies. The insets of (a) and (b) show the participation number (PN) $P(\omega)$ [Eq. (4)] for BLJ and bulk polymers at the same temperatures shown in the main panel.

associated with localized and delocalized modes that do not require a finite-size analysis. Delocalized modes are defined as those that involve an extensive fraction of the system, while localized modes involve an intensive fraction. This is quantified by the participation number (PN),

$$P_\omega = \left\langle \left(\sum_i (e_i^\omega \cdot e_i^\omega)^2 \right)^{-1} \right\rangle, \quad (4)$$

where e_i^ω is the contribution of particle i to the normalized eigenvector corresponding to eigenfrequency ω . We evaluate the participation number and show its frequency dependence in the insets of Fig. 1 for a single system size, which shows that the smaller values of the PN occur at the wings of the DOS, corresponding to localized modes. The transition frequency between localized and delocalized modes is known for the BLJ system from Ref. 11, and we examine three system sizes for the polymer system to identify the transition location of that system. By scaling the participation number by the linear system size $L \sim N^{1/3}$, i.e., $\bar{P}_\omega = P_\omega/L$ [shown in Figs. 2(a) and 2(c)], we see that the scaled participation number (\bar{P}) is L -invariant at the transition point. Transitions between localized and delocalized modes occur at two crossover frequencies: $\omega_c^{\text{unstable}}$ in the unstable region and ω_c^{stable} in the stable region. Accordingly, in Figs. 2(a) and 2(c), from left to right, the vibrational spectrum can be separated into unstable localized

(UL), unstable delocalized (UD), stable delocalized (SD), and stable localized (SL) modes. It is not surprising that the transition between localized and delocalized stable modes for the polymer system occurs at the same location as the dip in the DOS that separates the contributions to the DOS from the intramolecular bonds of the polymer.

B. INM clusters and their relation to extreme mobility clusters

The local mobility of glass-forming materials becomes increasingly dynamical heterogeneous below an onset temperature T_A , above which Arrhenius relaxation provides an adequate description of the fluid dynamics.³⁰ Particles with either significantly enhanced or suppressed mobilities form spatially correlated clusters. In this section, we examine the clusters of particles associated with the INM spectrum and compare these dynamical clusters with extreme high and low mobilities.

Having distinguished the different types of modes in the INM spectrum, we next examine the spatial correlations of particles in each mode. For the delocalized modes, all particles have a similar contribution to the PN so that the contribution of particle i to the participation number at frequency ω , i.e., $e_i^\omega \cdot e_i^\omega \approx 1/N$, by definition. For the localized modes, some particles make a much larger contribution to the PN, while others make a much smaller

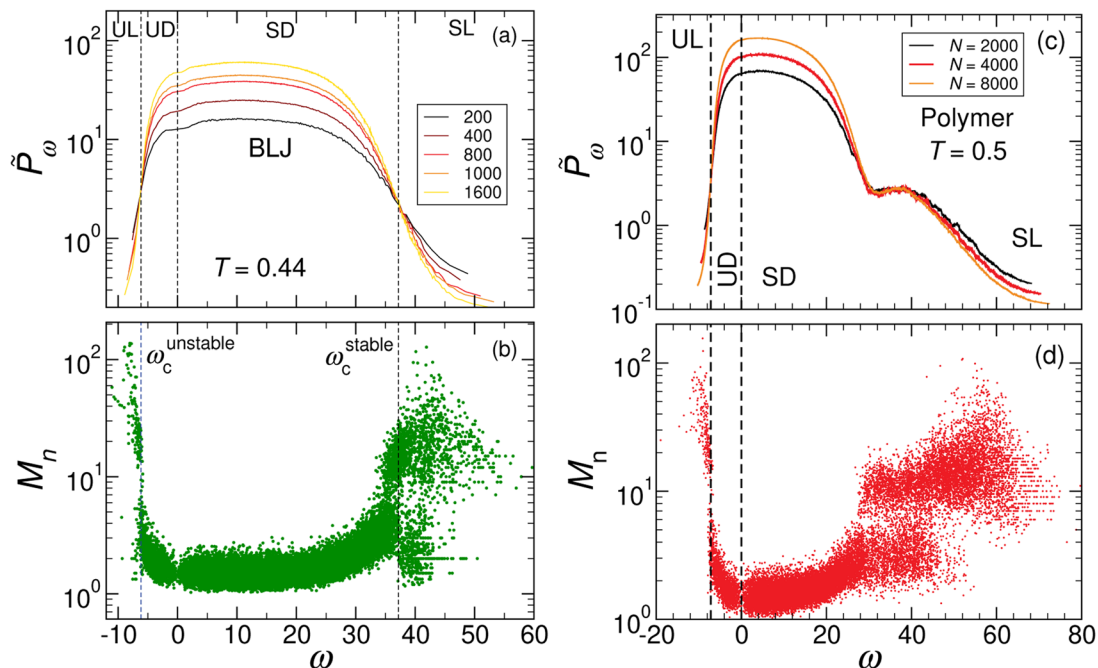


FIG. 2. The modified participation number $\bar{P}_\omega = P_\omega/L$ of (a) binary Lennard-Jones mixture and (c) polymer for various system sizes. The system size dependence study pinpoints the transition between localized and delocalized modes. From left to right, the figure shows the regions of unstable localized (UL), unstable delocalized (UD), stable delocalized (SD), and stable localized (SL), which are separated by the crossover point and marked by dashed lines. The average size of particle clusters M_n for each frequency ω for (b) BLJ and (d) polymer. The particles that contribute most to the mode ($e_i^\omega \cdot e_i^\omega > 1/N$) form spatially correlated clusters in the UL and SL modes. Thus, by studying the frequency dependence of the cluster sizes, we can identify the transition frequency $\omega_c^{\text{unstable}}$ and ω_c^{stable} without the need for a system-size dependent study. The transition frequency $\omega_c^{\text{unstable}}$ between localization and delocalization in the unstable modes can be identified by the critical cluster size $M_n = 10$ [$\omega_c^{\text{unstable}} \equiv \omega(M_n = 10)$].

contribution. Accordingly, a criterion $\mathbf{e}_i^\omega \cdot \mathbf{e}_i^\omega > 1/N$ identifies the particles that contribute most significantly to the PN. For each frequency ω , we examine the spatial correlation between these particles by evaluating the average cluster size M_n of these particles for all ω . We define two particles as part of the same cluster if the distance between these particles is less than a nearest-neighbor cut-off distance, defined by the location of the first minimum in the density-density pair correlation function $g(r)$; here, $r_{\min}^{\text{BLJ}} = 1.38$ and $r_{\min}^{\text{poly}} = 1.46$. Using this method, we identify particle clusters for each ω . Since it is possible to have multiple clusters at each frequency, we evaluate the number-averaged cluster size as a function of ω in Fig. 2(b) for BLJ and Fig. 2(d) for the polymer. Note that we exclude the clusters that fully span the simulation box with periodic boundary conditions since these clusters correspond to clusters having infinite size; this includes almost all clusters of the delocalized modes, leaving only very small clusters of delocalized modes. We find that the average cluster size M_n is significantly larger in UL and SL modes than that in UD and SD modes (Fig. 2). It is natural to expect the particles in localized modes to be clustered, though not a prerequisite.

An examination of cluster size offers a simple means to separate localized and delocalized modes. By comparing to the crossover defined from the finite-sized scaling of the PN [Figs. 2(b) and 2(d)], we can identify the transition frequency between unstable localized mode and unstable delocalized mode based on cluster size as $\omega_c^{\text{unstable}} \equiv \omega(M_n = 10)$ for both BLJ and polymer fluids, since below (or above) this characteristic system size, the INM spectrum delocalized (localized), regardless of the system size (not shown for clarity in this figure). Thus, we can identify the transition frequency $\omega_c^{\text{unstable}}$ between UL and UD modes (see Fig. S3 of the supplementary material for the temperature dependence of this transition frequency), and ω_c^{stable} between SD and SL modes by the behavior of cluster size using only a single system size. Note that in the case of polymer melts, the crossover between SD and SL cannot be assigned a single frequency but rather corresponds to a frequency band around 30, which defines the localization crossover. The avoidance of a finite-size study of INMs offers a substantial computational advantage, particularly since the evaluation of the eigenvectors is

computational time and memory intensive for much larger system sizes.

The UL modes exhibit spatially correlated clusters, as indicated by the relatively large average cluster size in the leftmost part of the spectrum [Figs. 2(b) and 2(d)]. We visualize some representative UL clusters from the polymer in Fig. 4(a). Evidently, these UL clusters are, indeed, highly spatially correlated and do not appreciably overlap at different frequencies. [Panels (b) and (c) of Fig. 4 are discussed later.] In the UL modes of the polymer fluid, the percentage of particles that make the most contribution to these modes (with $\mathbf{e}_i^\omega \cdot \mathbf{e}_i^\omega > 1/N$) ranges from less than 1% to about 5%, as ω increases toward zero frequency and is nearly invariant with temperature. Notably, this percentage is consistent with the inferred dynamics “initiator” concentration in the string model of glass-formation.^{31,32} Similarly, particles associated with the SL mode that contribute most to the PN also form spatially correlated clusters, as indicated by the cluster size $M_n \gtrsim 10$ in that region. In the remaining discussion, we focus on clusters of the UL modes, since these modes are naturally expected to be related to localized molecular rearrangements. The stable modes, on the other hand, should correspond to reversible vibrational motions. Of course, the localized stable modes may also involve low frequency “soft modes” corresponding to large scale collective oscillatory motions, involving an appreciable number of particles.^{50,51} We plan to focus on the geometric nature of the motions involved in these modes in a separate paper.

One of the most salient properties of dynamical heterogeneity in cooled liquids is the growth of spatially correlated clusters having extremely low or high mobility,³⁰ and we initially expected that INM clusters have some direct relationship to dynamically heterogeneous motion observed in previous simulations.³⁰ In particular, we anticipate that their sizes would grow upon cooling as well. Since we have already identified the frequency that separates the UL and UD modes for the polymer, we next examine the temperature T dependence of average cluster size in UL modes in Fig. 3. We find that the average cluster size in UL mode M_{UL} increases with decreasing T , reminiscent of both the mobile and immobile particle cluster sizes studied previously.³⁰

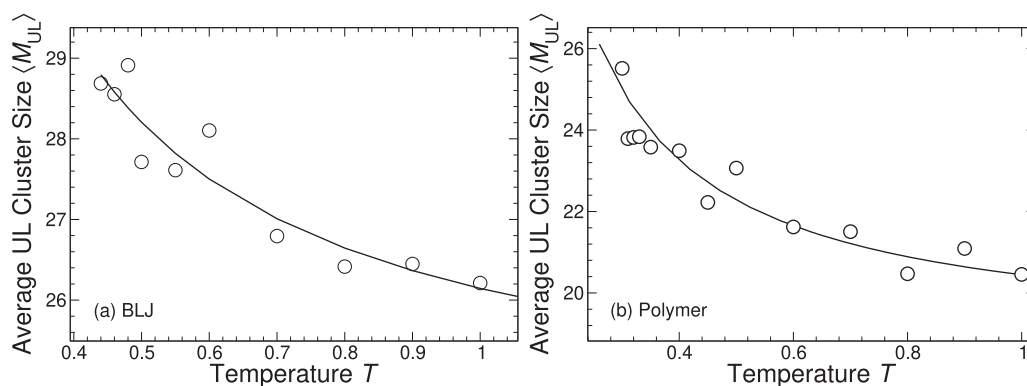


FIG. 3. The temperature dependence of the average size of UL clusters $\langle M_{\text{UL}} \rangle$ for (a) BLJ and (b) polymer. The size of UL clusters increases upon cooling, qualitatively similar to the dynamical clusters associated with extreme mobility. Solids curves are guides to the eye.

We now consider how these UL clusters might be related to clusters with extreme mobility. Since the size of the UL and mobility clusters is not comparable, we consider the characteristic lifetime of the UL clusters. In our previous work defining the characteristic lifetime of the mobile/immobile particle clusters,³⁰ we considered a certain fraction of particles at any given time interval from which particle clusters are identified and these particle clusters are subsequently normalized by the cluster size of a random collection of particles. (More details on the definitions of mobile and immobile particle clusters are provided in the [supplementary material](#) and Ref. 30.) It has been shown that the lifetime of the immobile particle evolves in a fashion that mirrors the collective intermediate scattering function and, unsurprisingly, the lifetime of the immobile particle can be essentially identified with the structural relaxation time τ_α .³⁰ In contrast, the mobile particles exhibit a lifetime comparable to the peak in the non-Gaussian parameter, a much shorter time in glass-forming liquids at low temperatures. Similarly, to quantify the persistence time of these UL particle clusters, we consider the relative displacement of these clusters. In particular, we evaluate the dimensionless displacement, $\langle \text{MSD}_{\text{clust}} \rangle / \langle \text{MSD} \rangle - 1$, where $\langle \text{MSD} \rangle$ is the mean square displacement for the particles in the system as a whole and $\langle \text{MSD}_{\text{clust}} \rangle$ is the mean square displacement for the UL particle clusters, weighted by the number of times these particles appear in the UL modes. We note that the fraction of particles that contribute most to the participation ratio in the UL modes is almost invariant with temperature.

In Fig. 5, we plot the measure of the relative mobility of UL clusters as a function of time for various T . Interestingly, for both the BLJ and polymer systems, the time scale of the peak values of the largest relative displacement of UL clusters grows upon cooling and occurs at a time scale well beyond that of the vibrational time scale for which the INM would naively be expected to persist. For the polymer case, we find two characteristic peaks—the first of which occurs at a time scale on the order of the vibrational time [$\mathcal{O}(10^{-13}\text{s})$] of the polymer, which is independent of T . The absence of such a peak in the BLJ system suggests that this is a polymer-specific effect associated with modes related to the bond potential. We point out that the mean-squared displacement of the particles in these UL clusters is only slightly larger than the system as a whole, indicating that these clusters cannot be identified with mobile particle clusters. To illustrate this more clearly, we follow previously established methods^{30,52} to identify the mobile and immobile particle clusters in polymers and compare these dynamical clusters to UL clusters. To illustrate this point visually, we render examples of the UL, mobile, and immobile clusters in space in Fig. 4. Specifically, we show representative UL clusters in panel (a) and mobile particle clusters in panel (b) and immobile particle clusters in panel (c) as red and blue beads. Evidently, the particle clusters in UL modes are spatially distinct from previously defined clusters having extreme mobility.

We now discuss the significance of this persistence time of UL clusters in relation to time governing the lifetime of the mobile and immobile particle clusters. To do so, we compare the characteristic lifetime t_{UL} of UL clusters to the lifetime of the mobile and immobile clusters.³⁰ As mentioned above, we define the lifetime of UL clusters t_{UL} as the time at which $\langle \text{MSD}_{\text{clust}} \rangle / \langle \text{MSD} \rangle - 1$ peaks (see Fig. 5). (We compare the relative size of the mobile and immobile particle clusters defined by Ref. 30 in Fig. S2 of the

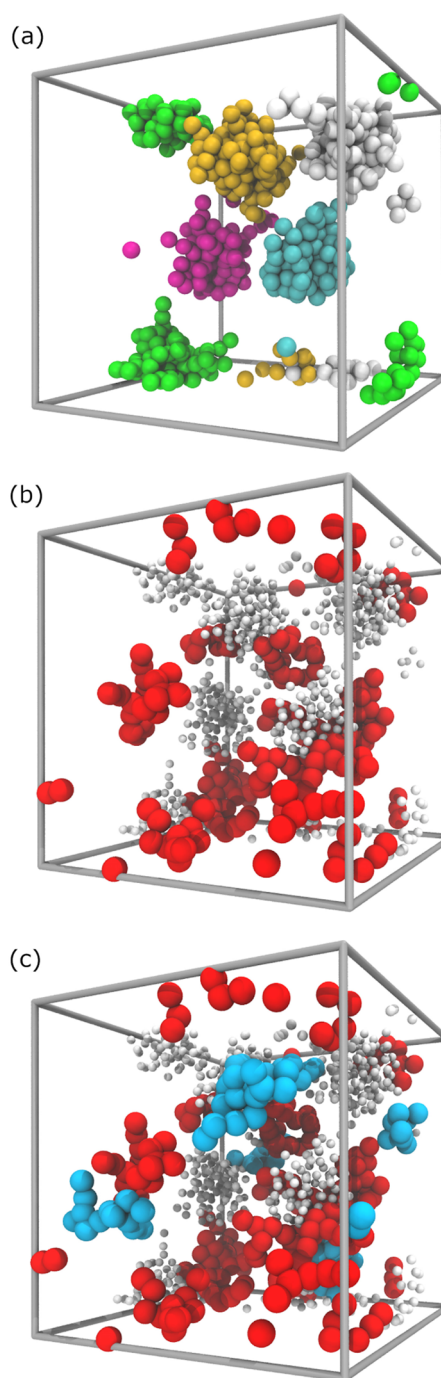


FIG. 4. Visualization of (a) some typical UL clusters in the polymer. Each color represents one frequency ω in the UL mode. (b) Clusters with excessively high mobility are rendered as red beads. We simultaneously superimpose the UL clusters from panel (a), rendered as small white beads. We see that UL clusters generally do not overlap strongly with the particle clusters having excessively high mobility. (c) Data from panels (a) and (b) are combined with the immobile particle clusters, which are rendered as blue beads. The configuration is taken from $T = 0.35$, and mobile and immobile particle clusters are identified at the time scale t_{UL} at which $\langle \text{MSD}_{\text{clust}} \rangle / \langle \text{MSD} \rangle - 1$ (Fig. 5) peaks.

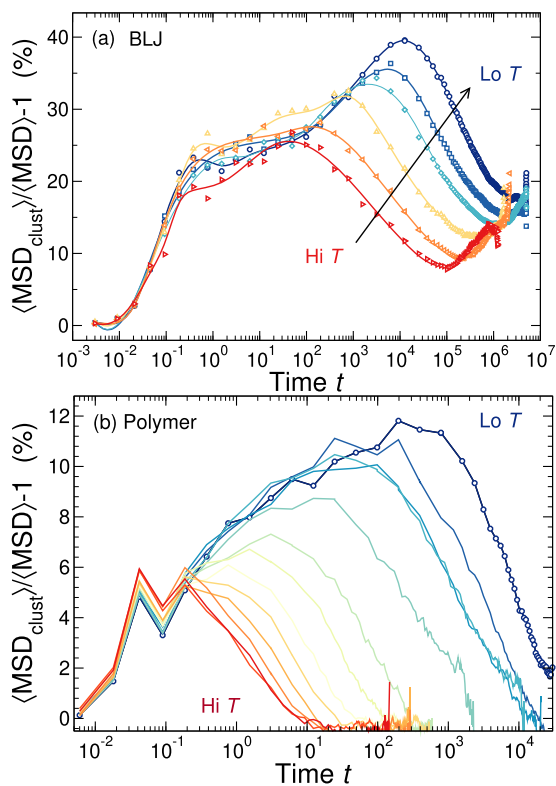


FIG. 5. The relative mean square displacement of UL clusters $\langle \text{MSD}_{\text{clust}} \rangle / \langle \text{MSD} \rangle - 1$ compared to that of all particles on average for (a) BLJ and (b) polymer.

supplementary material.) The characteristic times of these mobile t_M and immobile clusters t_I are correspondingly defined by the time at which the size of mobility clusters peaks. Figure 6 compares the characteristic times of mobile t_M , immobile t_I , and UL clusters t_{UL} , normalized by their values at the onset temperature T_A for glass formation. This eliminates the difference between the relaxation times associated with a simple constant prefactor.

We see from Fig. 6 that the normalized time t_{UL} nearly coincides with the normalized structural relaxation time τ_α obtained from the coherent intermediate scattering function at a scale of the interparticle distance (see Fig. S1 of the supplementary material). We also include the lifetime of the immobile particle clusters t_I , defined in our previous study,^{30,53} which scales proportionately to τ_α to a good approximation. Additionally, the lifetime of the mobile particle clusters t_M scales linearly with t^* , the characteristic time scale at which non-Gaussian parameter peaks.³⁰ Previous work has also shown that the characteristic time t_χ at which the 4-point density function peaks scales linearly with the structural relaxation time τ_α .⁵⁴ Consequently, we do not show t^* and t_χ in Fig. 6 due to the linear scaling with t_M and τ_α , respectively. The persistence of the UL clusters is clearly highly correlated with the persistence time of the immobile particle clusters, and thus the structural relaxation time τ_α and t_χ . The absolute value of the time scale t_{UL} is evidently shorter than either the mobile or immobile particles for the temperature range we investigate, but at the lowest

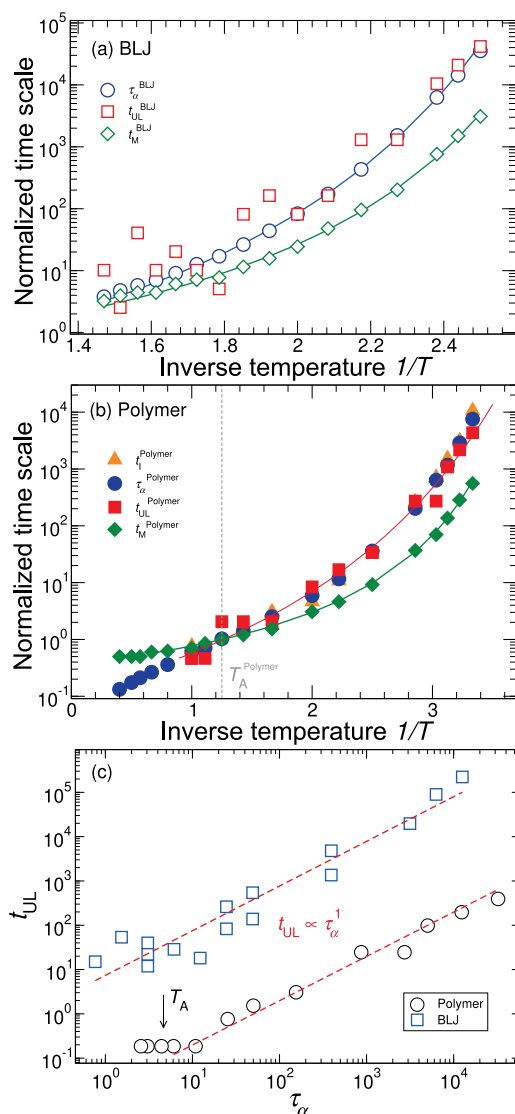


FIG. 6. Characteristic time scales for the peak cluster size of mobile, immobile, and UL modes, normalized by their values at T_A . Panel (a) shows data for BLJ, and panel (b) shows data for the polymer. There is a strong similarity between t_I (orange up triangles), t_{UL} (red squares), and τ_α (dark blue circles). (c) Parametric plot of the α -relaxation time τ_α and the characteristic time t_{UL} of the UL modes, demonstrating a linear proportionality between these characteristic time scales.

temperatures simulated, t_{UL} becomes similar to t_I . In particular, the lifetime t_{UL} of the UL modes grows linearly with the structural relaxation time τ_α to an excellent approximation. This relationship fully supports the hypothesis that the dynamic clusters associated with UL modes can be viewed as collective excitations, in accord with the theory of Zwanzig.⁴¹ This is the first direct evidence of the long-time persistence of the unstable mode in cooled liquids, although Zangi and Rice⁵⁵ and Coslovich and Pastore⁷ have previously suggested that such long term persistence of unstable modes might exist.

IV. CONCLUSIONS

Our analysis of the heterogeneous dynamics of a model polymer and metallic glass-forming liquids indicates that there are multiple distinct types of dynamical heterogeneities that contribute to the dynamics of glass-forming liquids. In previous work, we identified “mobile” and “immobile” particles having a significant influence on the rate of molecular diffusion and structural relaxation, respectively.³⁰ Both classes of particles form fractal clusters that grow upon cooling whose lifetimes are reflected in autocorrelation functions associated with molecular diffusion and the relaxation of density fluctuations in the fluid. The present work considers the proposed existence of long-lived collective excitations in model glass-forming liquids, and we provide evidence that the clustering particles associated with the unstable localized modes can be identified with well-defined large scale collective excitations.⁴¹ These localized modes are identified by a combination of an instantaneous mode analysis and methodology drawn from random matrix theory. We find that there is yet another clustering phenomenon associated with these collective excitations in the fluid. The unstable localized clusters are found to increase in size, similarly to the immobile and mobile particle clusters with decreasing temperature, but this new class of clusters is found to lie in the interfacial region between the previously defined “mobile” and “immobile” particle clusters. Along these lines, recent simulations have suggested a three-state dynamical heterogeneity in glass-forming liquids.⁴² Because our findings are also consistent between the Kob-Andersen model of metallic glass-forming liquids and polymer melts, we expect these results to be general. The unstable localized mode particle clusters evidently serve to *facilitate* the fluid relaxation process, but these clusters do not actually participate in the large scale collective motion associated with barrier crossing events governing activated transport.

Based on the observation of the present paper, we should also look for long-lived material excitations in cooled liquids by neutron scattering methods in the same fashion as for liquid ⁴He.^{56,57} In particular, these excitations should be evidenced by a material dispersion relation defined by a scattering peak in the dynamic structure factor as a function of wavevector q . At low q , a linear scaling of the $S(q, \omega)$ peak position, corresponding to the propagation of sound waves (phonons) associated with the localized stable modes, should be observed, while at higher q values, comparable to the interparticle spacing, we might expect a roton minimum in the dispersion relation, just as found in liquid ⁴He.^{56,57} Such a minimum has, in fact, been observed in the metallic glass ZnMg and other materials,^{58,59} where this feature is accessible experimentally by neutron scatterings.⁶⁰ This feature has also been greatly discussed in relation to understanding the low temperature dependence of the specific heat and thermal conductivity in glass-forming liquids.^{61–64} We tentatively suggest that the Boson peak of glass-forming liquids might be identified with the energy gap defining the excitation energy of the collective momentum fluctuations, an interpretation similar to the roton energy of liquid ⁴He.^{56,57}

SUPPLEMENTARY MATERIAL

See the [supplementary material](#) for details on the definition of relaxation time, mobile and immobile particle clusters, unstable mode fraction, and critical transition frequency.

ACKNOWLEDGMENTS

Computer time was provided by Wesleyan University. This work was supported in part by NIST (Award No. 70NANB13H202).

REFERENCES

- ¹A. Rahman, M. Mandell, and J. McTague, “Molecular dynamics study of an amorphous Lennard-Jones system at low temperature,” *J. Chem. Phys.* **64**, 1564–1568 (1976).
- ²S. D. Bembek and B. B. Laird, “The role of localization in glasses and supercooled liquids,” *J. Chem. Phys.* **104**, 5199–5208 (1996).
- ³T. Keyes, “Instantaneous normal mode approach to liquid state dynamics,” *J. Phys. Chem. A* **101**, 2921–2930 (1997).
- ⁴R. M. Strat, “The instantaneous normal modes of liquids,” *Acc. Chem. Res.* **28**, 201–207 (1995).
- ⁵A. Widmer-Cooper, H. Perry, P. Harrowell, and D. R. Reichman, “Localized soft modes and the supercooled liquid’s irreversible passage through its configuration space,” *J. Chem. Phys.* **131**, 194508 (2009).
- ⁶A. Chumakov, I. Sergueev, U. Van Bürck, W. Schirmacher, T. Asthalter, R. Rüffer, O. Leupold, and W. Petry, “Collective nature of the Boson peak and universal transboson dynamics of glasses,” *Phys. Rev. Lett.* **92**, 245508 (2004).
- ⁷D. Coslovich and G. Pastore, “Are there localized saddles behind the heterogeneous dynamics of supercooled liquids?,” *Europhys. Lett.* **75**, 784 (2006).
- ⁸M. Russina, F. Mezei, R. Lechner, S. Longeville, and B. Urban, “Experimental evidence for fast heterogeneous collective structural relaxation in a supercooled liquid near the glass transition,” *Phys. Rev. Lett.* **84**, 3630 (2000).
- ⁹W.-X. Li and T. Keyes, “Instantaneous normal mode theory of diffusion and the potential energy landscape: Application to supercooled liquid CS₂,” *J. Chem. Phys.* **111**, 5503–5513 (1999).
- ¹⁰T. Keyes, J. Chowdhary, and J. Kim, “Random energy model for dynamics in supercooled liquids: N dependence,” *Phys. Rev. E* **66**, 051110 (2002).
- ¹¹V. I. Clapa, T. Kottos, and F. W. Starr, “Localization transition of instantaneous normal modes and liquid diffusion,” *J. Chem. Phys.* **136**, 144504 (2012).
- ¹²B. Madan and T. Keyes, “Unstable modes in liquids density of states, potential energy, and heat capacity,” *J. Chem. Phys.* **98**, 3342–3350 (1993).
- ¹³S. D. Bembek and B. B. Laird, “Instantaneous normal modes and the glass transition,” *Phys. Rev. Lett.* **74**, 936 (1995).
- ¹⁴F. Sciortino and P. Tartaglia, “Harmonic dynamics in supercooled liquids: The case of water,” *Phys. Rev. Lett.* **78**, 2385 (1997).
- ¹⁵W.-X. Li and T. Keyes, “Pure translation instantaneous normal modes: Imaginary frequency contributions vanish at the glass transition in CS₂,” *J. Chem. Phys.* **107**, 7275–7277 (1997).
- ¹⁶W.-X. Li, T. Keyes, and F. Sciortino, “Three-flavor instantaneous normal mode formalism: Diffusion, harmonicity, and the potential energy landscape of liquid CS₂,” *J. Chem. Phys.* **108**, 252–260 (1998).
- ¹⁷J. D. Gezelter, E. Rabani, and B. Berne, “Can imaginary instantaneous normal mode frequencies predict barriers to self-diffusion?,” *J. Chem. Phys.* **107**, 4618–4627 (1997).
- ¹⁸C. Donati, F. Sciortino, and P. Tartaglia, “Role of unstable directions in the equilibrium and aging dynamics of supercooled liquids,” *Phys. Rev. Lett.* **85**, 1464 (2000).
- ¹⁹E. La Nave, A. Scala, F. W. Starr, F. Sciortino, and H. E. Stanley, “Instantaneous normal mode analysis of supercooled water,” *Phys. Rev. Lett.* **84**, 4605 (2000).
- ²⁰E. La Nave, A. Scala, F. W. Starr, H. Stanley, and F. Sciortino, “Dynamics of supercooled water in configuration space,” *Phys. Rev. E* **64**, 036102 (2001).
- ²¹J. Chowdhary and T. Keyes, “Conjugate gradient filtering of instantaneous normal modes, saddles on the energy landscape, and diffusion in liquids,” *Phys. Rev. E* **65**, 026125 (2002).
- ²²S. Sastry, N. Deo, and S. Franz, “Spectral statistics of instantaneous normal modes in liquids and random matrices,” *Phys. Rev. E* **64**, 016305 (2001).
- ²³S. Ciliberti and T. S. Grigera, “Localization threshold of instantaneous normal modes from level-spacing statistics,” *Phys. Rev. E* **70**, 061502 (2004).

- ²⁴T. Rieth and M. Schreiber, "The Anderson transition in three-dimensional quasiperiodic lattices: Finite-size scaling and critical exponent," *Z. Phys. B Condens. Matter* **104**, 99–102 (1997).
- ²⁵H. Sillescu, "Heterogeneity at the glass transition: A review," *J. Non-Cryst. Solids* **243**, 81–108 (1999).
- ²⁶R. Böhmer, G. Hinze, T. Jörg, F. Qi, and H. Sillescu, "Dynamical heterogeneity in α - and β -relaxations of glass forming liquids as seen by deuteron NMR," *J. Phys.: Condens. Matter* **12**, A383 (2000).
- ²⁷G. S. Matharoo, M. G. Razul, and P. H. Poole, "Structural and dynamical heterogeneity in a glass-forming liquid," *Phys. Rev. E* **74**, 050502 (2006).
- ²⁸K. Binder and W. Kob, *Glassy Materials and Disordered Solids: An Introduction to Their Statistical Mechanics* (World Scientific, 2011).
- ²⁹C. Donati, J. F. Douglas, W. Kob, S. J. Plimpton, P. H. Poole, and S. C. Glotzer, "Stringlike cooperative motion in a supercooled liquid," *Phys. Rev. Lett.* **80**, 2338 (1998).
- ³⁰F. W. Starr, J. F. Douglas, and S. Sastry, "The relationship of dynamical heterogeneity to the Adam-Gibbs and random first-order transition theories of glass formation," *J. Chem. Phys.* **138**, 12A541 (2013).
- ³¹B. A. Pazmiño Betancourt, J. F. Douglas, and F. W. Starr, "String model for the dynamics of glass-forming liquids," *J. Chem. Phys.* **140**, 204509 (2014).
- ³²W. Zhang, F. W. Starr, and J. F. Douglas, "Collective motion in the interfacial and interior regions of supported polymer films and its relation to relaxation," *J. Phys. Chem. B* **123**, 5935–5941 (2019).
- ³³K. Vollmayr-Lee, W. Kob, K. Binder, and A. Zippelius, "Dynamical heterogeneities below the glass transition," *J. Chem. Phys.* **116**, 5158–5166 (2002).
- ³⁴K. Vollmayr-Lee and A. Zippelius, "Heterogeneities in the glassy state," *Phys. Rev. E* **72**, 041507 (2005).
- ³⁵J. C. Conrad, P. P. Dhillon, E. R. Weeks, D. R. Reichman, and D. A. Weitz, "Contribution of slow clusters to the bulk elasticity near the colloidal glass transition," *Phys. Rev. Lett.* **97**, 265701 (2006).
- ³⁶U. R. Pedersen, T. B. Schröder, J. C. Dyre, and P. Harrowell, "Geometry of slow structural fluctuations in a supercooled binary alloy," *Phys. Rev. Lett.* **104**, 105701 (2010).
- ³⁷A. Anikeenko and N. Medvedev, "Polytetrahedral nature of the dense disordered packings of hard spheres," *Phys. Rev. Lett.* **98**, 235504 (2007).
- ³⁸H. Tanaka, T. Kawasaki, H. Shintani, and K. Watanabe, "Critical-like behaviour of glass-forming liquids," *Nat. Mater.* **9**, 324 (2010).
- ³⁹W. Zhang, J. F. Douglas, and F. W. Starr, "Dynamical heterogeneity in a vapor-deposited polymer glass," *J. Chem. Phys.* **146**, 203310 (2017).
- ⁴⁰G. Tarjus and D. Kivelson, "Breakdown of the Stokes–Einstein relation in supercooled liquids," *J. Chem. Phys.* **103**, 3071–3073 (1995).
- ⁴¹R. Zwanzig, "Elementary excitations in classical liquids," *Phys. Rev.* **156**, 190 (1967).
- ⁴²T. Das and J. F. Douglas, "Quantifying structural dynamic heterogeneity in a dense two-dimensional equilibrium liquid," *J. Chem. Phys.* **149**, 144504 (2018).
- ⁴³A. S. Keys, L. O. Hedges, J. P. Garrahan, S. C. Glotzer, and D. Chandler, "Excitations are localized and relaxation is hierarchical in glass-forming liquids," *Phys. Rev. X* **1**, 021013 (2011).
- ⁴⁴T. Kawasaki and A. Onuki, "Dynamics of thermal vibrational motions and stringlike jump motions in three-dimensional glass-forming liquids," *J. Chem. Phys.* **138**, 12A514 (2013).
- ⁴⁵T. Kawasaki and A. Onuki, "Slow relaxations and stringlike jump motions in fragile glass-forming liquids: Breakdown of the Stokes–Einstein relation," *Phys. Rev. E* **87**, 012312 (2013).
- ⁴⁶H. Zhang, C. Zhong, J. F. Douglas, X. Wang, Q. Cao, D. Zhang, and J.-Z. Jiang, "Role of string-like collective atomic motion on diffusion and structural relaxation in glass forming Cu–Zr alloys," *J. Chem. Phys.* **142**, 164506 (2015).
- ⁴⁷T. S. Ingebrigtsen, J. C. Dyre, T. B. Schröder, and C. P. Royall, "Crystallization instability in glass-forming mixtures," *Phys. Rev. X* **9**, 031016 (2019).
- ⁴⁸W. Kob and H. C. Andersen, "Testing mode-coupling theory for a supercooled binary Lennard–Jones mixture I: The van Hove correlation function," *Phys. Rev. E* **51**, 4626 (1995).
- ⁴⁹G. S. Grest and K. Kremer, "Molecular dynamics simulation for polymers in the presence of a heat bath," *Phys. Rev. A* **33**, 3628 (1986).
- ⁵⁰M. L. Manning and A. J. Liu, "Vibrational modes identify soft spots in a sheared disordered packing," *Phys. Rev. Lett.* **107**, 108302 (2011).
- ⁵¹A. Smessaert and J. Rottler, "Structural relaxation in glassy polymers predicted by soft modes: A quantitative analysis," *Soft Matter* **10**, 8533–8541 (2014).
- ⁵²Y. Gebremichael, T. Schröder, F. W. Starr, and S. Glotzer, "Spatially correlated dynamics in a simulated glass-forming polymer melt: Analysis of clustering phenomena," *Phys. Rev. E* **64**, 051503 (2001).
- ⁵³N. Lačević, F. W. Starr, T. Schröder, and S. Glotzer, "Spatially heterogeneous dynamics investigated via a time-dependent four-point density correlation function," *J. Chem. Phys.* **119**, 7372–7387 (2003).
- ⁵⁴W.-S. Xu, J. F. Douglas, and K. F. Freed, "Influence of cohesive energy on relaxation in a model glass-forming polymer melt," *Macromolecules* **49**, 8355–8370 (2016).
- ⁵⁵R. Zangi and S. A. Rice, "Instantaneous normal modes and cooperative dynamics in a quasi-two-dimensional system of particles," *J. Phys. Chem. B* **108**, 6856–6865 (2004).
- ⁵⁶W. Montfrooij, E. Svensson, I. De Schepper, and E. Cohen, "Effective eigenmode description of normal and superfluid ^4He ," *J. Low Temp. Phys.* **109**, 577–623 (1997).
- ⁵⁷W. Montfrooij and E. Svensson, "Phonons and rotons in liquid ^4He near the superfluid transition," *Physica B* **241**, 924–928 (1997).
- ⁵⁸J.-B. Suck, H. Rudin, H.-J. Güntherodt, and H. Beck, "Short-wavelength transverse collective modes in a metallic glass," *J. Phys. C: Solid State Phys.* **13**, L1045 (1980).
- ⁵⁹P. Randolph and K. Singwi, "Slow-neutron scattering and collective motions in liquid lead," *Phys. Rev.* **152**, 99 (1966).
- ⁶⁰J.-B. Suck, H. Rudin, H.-J. Güntherodt, and H. Beck, "Experimental investigation of the dispersion of collective density fluctuations near Q_p in a metallic glass," *Phys. Rev. Lett.* **50**, 49 (1983).
- ⁶¹N. Kovalenko and Y. P. Krasny, "On the low temperature anomaly of metal glass heat capacity I," *Physica B* **162**, 115–121 (1990).
- ⁶²N. Astrath, M. Baesso, A. Bento, C. Colucci, A. Medina, and L. Evangelista, "Phonon–roton-like elementary excitations and low-temperature behaviour of non-crystalline solids," *Philos. Mag.* **86**, 227–235 (2006).
- ⁶³S. Takeno and M. Goda, "A theory of phonon-like excitations in non-crystalline solids and liquids," *Prog. Theor. Phys.* **47**, 790–806 (1972).
- ⁶⁴S. Takeno and M. Goda, "Frequency spectrum and low-temperature specific heat of noncrystalline solids," *Prog. Theor. Phys.* **48**, 1468–1473 (1972).